Fire Technology

Manufactured in The United States
https://doi.org/10.1007/s10694-023-01523-3

Repeat Fire Tests of Upholstered Furniture: Variability and Experimental Observations

*David Morrisset**, *Jonathan Reep*, *Ian Ojwang*, *Rory M. Hadden* and *Angus Law*, *School of Engineering, The University of Edinburgh, Edinburgh, UK*

Received: 21 June 2023/**Accepted:** 20 November 2023

Abstract. A series of trials were conducted to investigate the repeatability of furniture-scale calorimetry experiments. Twenty-five identical upholstered chairs were ignited under the same experimental conditions. Experimental results of heat release rate (HRR), mass loss rate (MLR), and emission yields (CO, CO_2, N_2O, NO, CH_4, HCN) are presented. Discrepancies were observed between the time resolved evolution of the various recorded data. However the development of each fire was observed to be tied to common events. By accounting for these events, a more consistent representation of the burning behaviour can be expressed. Each experiment displayed distinct burning regimes (i.e., pyrolysis, flaming, and smouldering) which were identified through visual observation and through analysing the emission data. Some species yields were found to be approximately constant over some burning regimes (e.g., CO_2 yield over the flaming regime) while others displayed highly transient behaviour (e.g., CO yield was found to be burning regime dependent). Results from upholstered furniture scale experiments, including HRR and emission yields, are commonly used in various engineering applications; this study lends insight into the variability that can be observed for such data and the implications in applying this data in further analysis.

Keywords: Flammability, Furniture calorimetry, Polyurethane foam, Heat release rate, Large scale, Statistical uncertainty

1. Introduction

Upholstered furniture has been the subject of both regulatory fire testing [1, 2] and novel experimentation for many decades [3–5]. While bench-scale test methods, such as the Cone Calorimeter [6], provide valuable insight into material characteristics, complex products and assemblies are often tested at a larger scale to demonstrate fire performance. As such, furniture-scale calorimetry is a commonly used method for characterizing metrics such as fire size or species generation of larger products, including upholstered furniture [4].

* Correspondence should be addressed to: David Morrisset, E-mail: d.morrisset@ed.ac.uk

Published online: 25 January 2024

A previous review of the flammability literature reveals that experiments conducted at the bench scale are typically repeated in relatively small trial quantities (e.g., $n \leq 3$) [7]. It was found that even within a controlled testing scenario, such as the Cone Calorimeter, there can be a substantial degree of statistical variation for such flammability tests (i.e. upwards of 30% error in instantaneous mass loss rate data) [7, 8]. A much larger number of trials (e.g. $n > 10$) may be required to obtain the desired level of statistical certainty. At the furniture-scale, calorimetry data on heat release rate (HRR) is readily found in the literature for products and assemblies such as upholstered furniture [4, 9]. It is self-evident that, as the overall complexity of a system increases, experiments conducted on assemblies and products are likely to result in higher degrees of stochastic variation between trials. However, in most cases such data are presented for a single trial — or in some instances, trials conducted in triplicate [9, 10]. The degree of variability between trials conducted at the furniture-scale is therefore not well-understood.

An understanding of the statistical variation in such large-scale calorimetry data has direct implications for many engineering analyses which utilise metrics such as HRR as inputs. To the knowledge of the authors, no study has presented the results of 25 + repeat trials for upholstered furniture with the explicit aim of characterizing statistical variation. Recognising the utility of commonly reported data, such as HRR, the aim of this study is to experimentally investigate the variation and commonality observed across a large sample size of upholstered furniture experiments (i.e., $n = 25$).

2. Background

More than half a century of research has been dedicated to mitigating the hazards presented by upholstered furniture [3]. Babrauskas and co-authors [3, 4, 9, 11, 12] provide a comprehensive background to furniture flammability; this study will not, therefore, review the literature in its entirety. Recent studies have presented results of modern furniture fire performance (e.g., [13, 14]). A difference has been observed between furniture with high portions of synthetic materials such as polyurethane (PU) foam (referred to as "modern" furniture in the literature), compared to "legacy" furniture that contains primarily materials such as wood and cotton [15]. These studies have suggested that on average, "modern" furnishings cause faster fire growth and higher peak HRRs. "Modern" furniture therefore tends to present a greater fire hazard than "legacy" furniture. Additional research has been dedicated to investigations of PU foam, which is the major component in many "modern" upholstered furniture items (e.g., [16–18]).

Of particular note in the context of furniture-scale calorimetry is the recent work of the National Institute of Standards and Technology (NIST) in the US. This group has produced a series of recent publications that outline the fire performance of upholstered furniture and describe techniques to mitigate the burning of upholstered chairs [10, 19–23]. These studies have identified various aspects that influence the growth rate of upholstered furniture fires (e.g., generation of a pool fire beneath the item) and present a range of solutions to improve furniture safety,

such as passive fabric barriers within the make-up of the item which can greatly reduce the peak HRR. The studies presented by researchers at NIST also identify key physical events that occur over the duration of a given experiment and then highlight these events within the data [24]. The full-scale experiments in these studies were primarily conducted in triplicate, which is a higher sample size compared to much of the other literature.

The importance of physical events in the resulting fire behaviour is notable because it shows that changes in the measured data have origins in observable events. For example, these studies note a substantial increase in the HRR after the bottom membrane of the chair fails which then produces a large pool fire. This suggests that variability in the time resolved data for such trials can be explained, at least in part, by identifying physical events.

A recent study conducted by Zulmajdi et al. compiled distributions of HRR results taken from the literature for various fuel packages (e.g., upholstered chairs) [25]. While these compiled data provide a range of values found in the literature, the constituent results still focus on a low number of repeat trials and therefore does not directly address the variability for a single experimental configuration.

In general, statistical variability at the furniture-scale has been a subject of minimal investigation in the fire safety community. At the bench scale, statistical uncertainty was illustrated by a previous study [7]. The statistical variation of commonly reported Cone Calorimeter results (time to ignition and mass loss rate) was analysed for a sample size of $n = 100$ trials. It was found that the appropriate number of repeat trials was dependent on both the experimental conditions and target degree of certainty defined by the researchers. However, even for the relatively simple experiments of black PMMA in the Cone Calorimeter, it was found that an appreciable degree of statistical uncertainty remained for low trial quantities (e.g., $n < 5 - 10$) in some cases.

At a larger scale, Melcher et al. conducted compartment scale experiments with a high number of repeats (e.g., $n \geq 20$) [26]. They found high levels of uncertainty (i.e., variations of 50% to 70% of the mean) in burning rate (MLR) measurements and measurements of gas species (CO and CO_2) for even relatively "simple" compartment fire experiments. These results also highlight that the period of fire growth and decay showed the highest degree of variability in time. No equivalent statistical study has been conducted for experiments on the scale of furniture calorimetry.

2.1. Characterizing Burning Behaviour

Literature most commonly describes the fire size of a burning fuel package using the metric of HRR measured by oxygen consumption calorimetry [27]. An alternative method for obtaining the time resolved fire size is to measure the mass loss of the fuel and compute the mass loss rate (MLR). This metric captures the rate at which a fuel pryolyzes (i.e., mass burning rate), but it also captures a range of other phenomena not directly related to pyrolysis (e.g., moisture loss, char oxidation) [28, 29]. The MLR can then be multiplied by an effective heat of combustion

($\Delta H_{c,eff}$) to approximate the HRR. The MLR and HRR capture variations over time, and can therefore capture the response of the burning rate to various events during an experiment.

Other aspects of burning behaviour are associated with the generation of combustion products (e.g., CO, HCN). The combustion of solid fuels generates a wide range of gaseous products through the pyrolysis process, gas-phase oxidation (i.e., flaming), and solid-phase oxidation (i.e., smouldering). The generation of different emission species are dependent on the transition between these regimes of pyrolysis, flaming, and smouldering [30]. For example, the pyrolysis of the various materials found in upholstered furniture produce specific gaseous species (e.g., characterized by high production rates of CO). However once ignited, a significant portion of the pyrolysis gases are oxidized by the flame. In the case of CO, much of the CO generated from pyrolysis is oxidized by the flame to form CO_2 once ignited, resulting in a low CO yield during flaming [30].

Ultimately, flaming ceases as the fire decays and solid-phase char oxidation (smouldering) becomes increasingly dominant [31, 32]. In the smouldering regime, the production rate of many species changes. The species yield can be determined as $y_i = \dot{m}_i/\dot{m}_p$ or the mass generation rate of a species (i) divided by the mass loss rate. The species yield presents a rate of generation per unit mass of fuel consumed and serves as a key result from calorimetry experiments. Species yields are readily found in literature such as the SFPE handbook [33] and are often assumed as constant in practical applications (e.g., CFD modelling [34]). Identifying the rate at which a fuel generates various combustion products is therefore important in both engineering applications and in the general characterization of material burning behaviour.

The total uncertainty of any measurement is a combination of both the measurement error and statistical variation between trials. Measurement uncertainty for large-scale calorimetry is outlined in detail elsewhere [35]; the total combined uncertainty in metrics such as the HRR are laboratory dependent but at the furniture-scale can be approximated in the range$\sim$5% to 10%. It should be noted that for HRR calorimetry, there is also some uncertainty in the ability to resolve short duration events. This uncertainty is caused by the time between the release of the combustion products and the effluent reaching the gas analyser. Therefore capturing transient behaviour over very small intervals in time (i.e., on the order of seconds) introduces further uncertainty. The magnitude of the variation between trials conducted in this study will be shown to be characteristically greater than that of the measurement uncertainty alone. Trends in the transient HRR behaviour will generally focus on intervals sufficiently long to mitigate the uncertainty introduced by the gas analyser time delay (i.e., changes in the HRR over intervals greater than 30 s).

3. Experimental Methodology

Twenty-five identical chairs were ignited under a 1 MW calorimetry hood. The subsequent fire behaviour was quantified using a variety of measurements. The following sections describe the experimental method adopted for all twenty-five trials conducted.

3.1. The Chair

Twenty-five commercially available, identical, flat-packed upholstered chairs were acquired for this study. This fuel package was selected as a widely available upholstered chair in the UK market. Each chair consisted of two rear legs (22 cm height), two front legs (24 cm height), a seat cushion (47×58 cm) and a backrest (60×44 cm); the dimensions of the upholstered chair are outlined in Fig. 1. On inspection, the chair legs were found to be manufactured from wood, and both the seat cushion and backrest were framed using oriented strand board (OSB). The soft upholstery was comprised of polyurethane foam (PU foam), and covered with a polyester cover material (per the manufacture specifications). The total mass of the chair was approximately 11.65 kg (±1.5%) with approximately 20% of the mass being synthetic polymers. The relative mass of each constituent component can be found in Table 1. Each chair was assembled immediately prior to each experiment and in accordance with the manufacture's instructions; therefore as far as the authors are aware, the composition and assembly of each item is assumed to be identical.

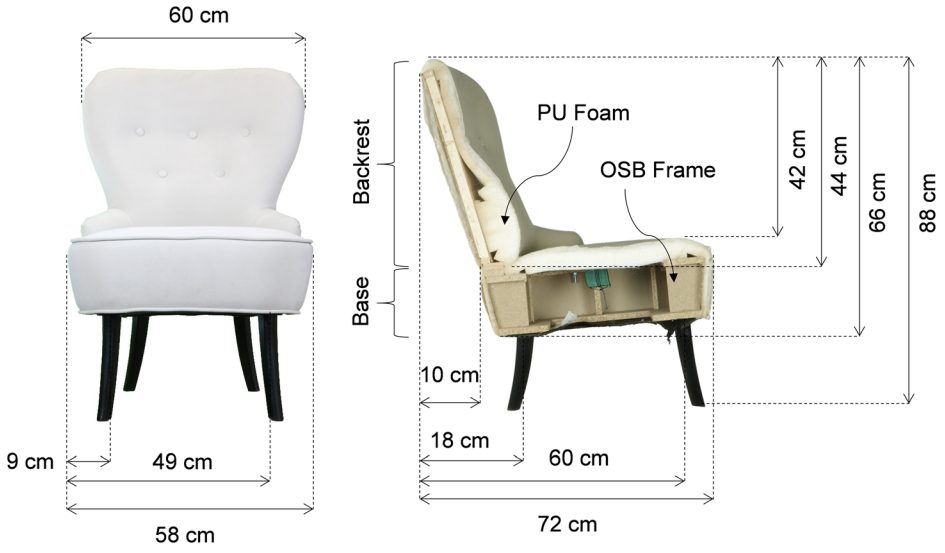

Figure 1. A cross section and front view of the chair used in this study.

Table 1
Relative Mass Contribution for Each of the Components in the Chair Used

Component	Mass (kg)	% Mass
PU foam	1.00	9
Misc. synthetic	1.05	9
OSB frame	8.22	72
Misc. wood	1.10	10

Only a single chair was sampled for components. However given the variation between chair masses was approximately 1.3% of the total mass, the mass percentages are assumed to be characteristic of all the chairs used in this study

3.2. The Ignition Source

Previous work on the burning of furniture shows that the choice of ignition source is of great importance for subsequent fire development [36]. Studies in the literature typically utilize a relatively large ignition source, such as the commonly used CA TB 133 18 kW burner [1, 2] with other standard burner sizes ranging upwards of 100 kW [37]. While such large ignition sources can be beneficial in standardized applications, a large ignition source dominates the initial phase of fire growth and masks potential stochastic variations seen with smaller ignition sources (stochastic variations that are relevant in realistic fire growth).

Therefore a small ignition source was used in this study. A 0.7 kW premixed propane burner (nominal flow of 0.015 g/s of propane) was selected as the ignition source for this study. The flow rate was controlled from a mass flow controller, and the burner flame was adjusted to be 15 cm in length for each trial. Initial experiments (using additional chairs) were conducted in an attempt to explore different ignition locations. The same burner was used to directly impinge on the chair at various locations (e.g., front of the seat cushion, base of the backrest from behind) however, these locations did not result in sustained burning.

It was found that the chair could be consistently ignited if the burner was placed beneath and in the centre of the seat cushion for 120 s. The burner was placed on a retractable mount such that the flame directly impinged on the underside of the chair. After 120 s, the burner was retracted and the fire allowed to develop without any other intervention. This ignition method was selected as it was judged to provide a balance between a reliable ignition process without the ignition source dominating the growth rate.

3.3. Instrumentation

Time resolved burning rates were captured through both the MLR and HRR. Gaseous emissions were recorded through two methods of gas analysis and collectively measured O_2, CO, CO_2, N_2O, NO, CH_4, and HCN.

All experiments were conducted beneath a 1 MW furniture calorimeter with a testing area of 2.5×2.5 m. The extraction hood was operated at a nominal flow of 1000 L/s for all experiments and was fitted with instrumentation for Oxygen Con-

sumption Calorimetry (OCC) measurements. Gas analysis was conducted using a Servomex 4100 Series gas analyser with CO and CO_2 measurements using inline spectroscopic analysis and O_2 measurements using paramagnetic cells. The intrinsic error of the analyser is reported as 0.2%, 0.1%, and 0.01% for O_2, CO_2, and CO respectively. Sample gases (N_2O, NO, CH_4, and HCN) from the calorimetry exhaust were analysed using Fourier-Transform Infrared Spectroscopy (FT-IR). A heated sampling line transported exhaust gas from the extraction location to the FT-IR. Analysis was conducted using a Gasmet DX4000 portable gas analyzer. Sample mass was recorded over the duration of the experiment using a Mettler Toledo Model PFK988-C300 load cell with a readout precision of 0.001 kg. Smoothing filters for the MLR data were chosen to mitigate temporal and magnitude distortion effects as identified in previous studies [29, 38]; more detail on smoothing filter selection can be found in the Appendix.

4. Results

Figure 2 shows the HRR results for each of these 25 trials. In each case the fire grew to a peak, and then decayed. The time at which the peak occurred varied between 308 and 745 s. The highest recorded peak HRR was 320 kW, and the lowest recorded peak HRR was 145 kW. Inspection of Fig. 2 reveals an envelope of HRR data showing a general increase to a peak HRR followed by a decay. Interpretation of these data requires understanding of the events associated with the burning of the chair, and the impact that these events may have on fire development. The following sections will systematically identify the events and physical drivers of each experiment to better contextualize the observed scatter.

4.1. Comparison of Two Trials

The results from two individual trials will first be described in detail to illustrate the key events and how these events affect the burning rate. While the following only focuses on two particular trials, the events that have been highlighted are based on an analysis of all trials conducted. The key events identified in this study are presented in Table 2, and illustrated in Fig. 3.

Figure 3 illustrates each key event during two different trials. While the key events are described in more detail within Tables 2 and 3, there are a few key observations in the data that can be tangibly linked to the occurrence of these events. The period between the burner being removed and the ignition of the backrest is characterized by horizontal flame spread along the upper surface of the cushion. Therefore the rate of growth in the HRR is relatively slow; however, once the backrest has ignited, the upward flame spread over the surface of the backrest leads to an increase in the HRR. The final growth to a peak HRR is initiated once flames are observed to break through the back surface of the chair which 1) indicated that all of the foam within the backrest was becoming involved in the fire and 2) allowed for a second surface for upwards flame spread. After the main peak, there are subsequent local increases in the HRR associated with mechanical failure of the chair backrest, and collapse of the OSB base. These

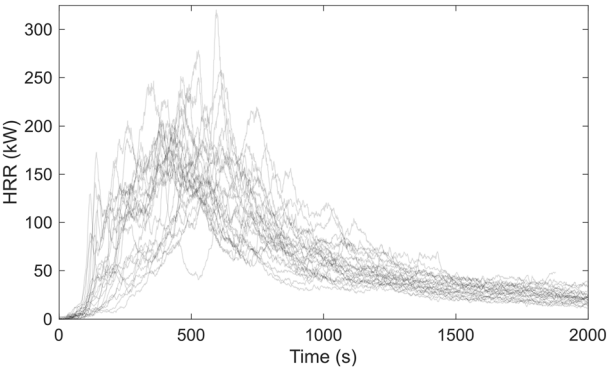

Figure 2. The HRR data recorded across all 25 trials under the same ignition conditions, presented to illustrate the variation between trials.

Table 2
Key Events Identified Across each Experiment

Event	Description of event
1. Burner Removed	Ignition burner removed after 120 s. The flame then spreads horizontally along the upper surface of the seat cushion
2. Backrest Ignition	Once the fabric of the backrest ignites, flames spread up the backrest leading to an increase in HRR
3. Flame Spread over the Backrest	Flames spread upwards along the backrest surface and display an increasing HRR. In most cases there was a distinct difference between ignition, flame spread to the top of the backrest, and spread over the entire backrest. All times identified in the table signify the point at which flames covered the entire front surface of the backrest
4. Burn-through of the Backrest	Between the backrest igniting and the peak HRR, flames were observed to have burned through the outermost cover of the backrest. At this point, all of the PU foam in the backrest became involved in the fire and there was rapid growth to the peak HRR
5. Peak HRR	The peak HRR was achieved once all remaining PU foam and synthetic material became involved
6. Collapse of the Backrest	Shortly after the peak, the HRR rapidly decreased as the synthetic combustibles were consumed leaving only the OSB frame of the chair remaining. The OSB frame supporting the chair ultimately chars and weakens to a point at which the backrest frame collapses. The collapse resulted in an instantaneous increase in the HRR as virgin OSB material was exposed and ignited
7. Collapse of the Base	In many trials, the OSB frame base of the chair remained intact after the backrest had detached from the remaining frame. Therefore the base itself collapsed at a later time leading to an additional instantaneous increase in HRR
8. Localised Flaming and Smouldering	After the frame collapses, the chair remains no longer displaying any resemblance to the original chair and show localised flaming and smouldering

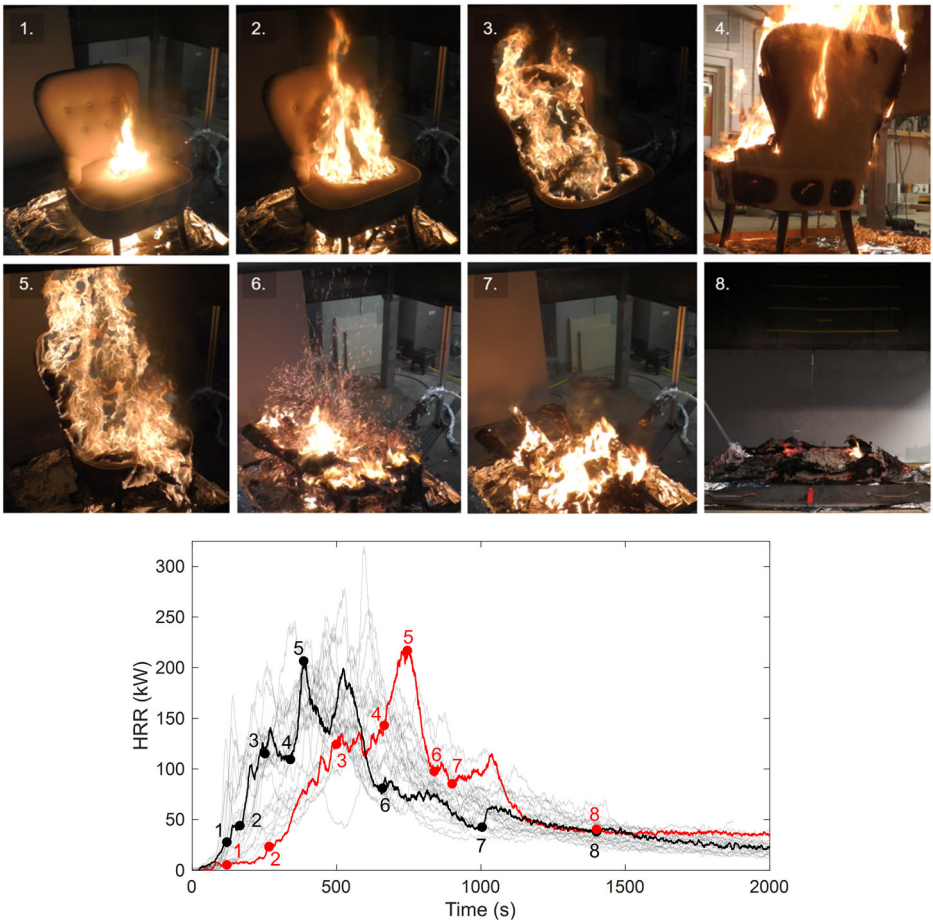

Figure 3. Outline of key events in time over the duration of the experiments conducted.

events expose fresh material (i.e., uncharred) which was then able to burn. After each collapse, the remaining material experienced only localized flaming and showed signs of smouldering. This analysis shows that Trial 2 cannot be simply seen as an "outlier" of the data set; instead, each event described in Table 2 can be linked to a direct influence on the observed HRR. While each event may occur at different times between trials, the subsequent effects on the HRR are consistent as seen when comparing Trial 1 and Trial 2 in Fig. 3.

Without knowledge of the events described in Table 2, the behaviours observed in the HRR data could not be explained. However, identifying these key events and tying them to the subsequent increase or decrease in HRR provide insight into the physical processes that governed the burning behaviour of the tested item. These stochastic events are likely unique to the upholstered chair used in this

Table 3
A Comparison of the Times and HRR Values at each Key Event Between the Two Trials Described in Fig. 3

	1. Burner removed		2. Backrest ignition		3. Flame spread over the backrest		4. Burn through of the backrest	
	Time (s)	HRR (kW)	Time (s)	HRR (kW)	Time (s)	HRR (kW)	Time (s)	HRR (kW)
Trial 1	120	27.7	165	44.0	252	115.2	340	109.5
Trial 2	120	5.5	266	23.3	500	124.5	665	143.1

	5. Peak HRR		6. Collapse of the backrest		7. Collapse of the base		8. Smouldering	
	Time (s)	HRR (kW)	Time (s)	HRR (kW)	Time (s)	HRR (kW)	Time (s)	HRR (kW)
Trial 1	386	206.5	659	81.0	1004	42.5	> 1200	51 to 21
Trial 2	745	216.9	838	97.7	900	85.4	> 1200	52 to 35

study. Other assemblies and products will express different observable events that influence the burning rate. However, these events illustrate the need for the time resolved burning rate of complex fuel items to be carefully tied to observed events to better interpret the recorded data. As noted above, every event identified was observed in every trial; while the observed HRR trends between trials may vary, the physical drivers for the resulting HRR were consistent across each trial.

4.1.1. Burning Regimes The key events identified above are important for interpretation of the burning rate data. Further insight into the generation of gaseous emissions can be gained by considering the burning regimes identified previously (i.e., pyrolysis, flaming, smouldering). These regimes of burning can be seen in Fig. 4, showing the MLR and CO results from an individual trial. Each burning regime can be characterised as follows:

- Pyrolysis regime: Indicated by a significant release of pyrolysis gas, but relatively little flaming. This was reflected by the increasing mass loss rate, and increasing concentrations of CO within the exhaust gases.
- Flaming regime: Indicated by a decrease in the measured concentrations of CO due to the oxidation of CO to CO_2.
- Smouldering regime: Indicated by the decline in the burning rate, but a continued increase in CO yield.

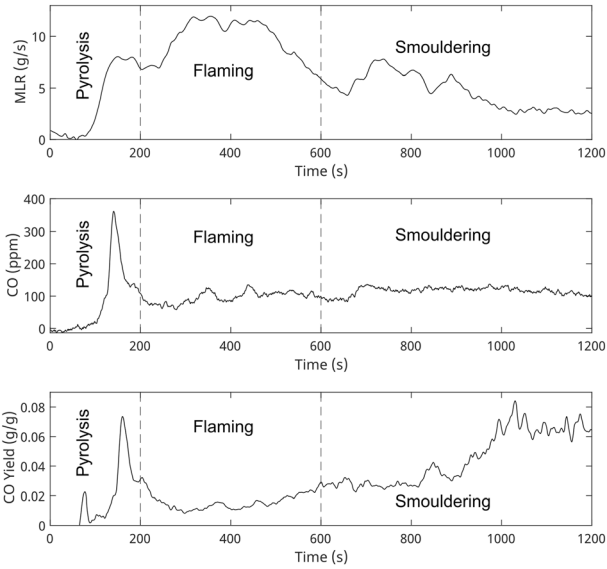

Figure 4. The global burning regimes for an experiment. (1) high rates of pyrolysis with minimal flaming, (2) flaming combustion, and (3) localized flaming and smouldering combustion.

How the eight key events fit within and precipitate these regimes is of interest in characterizing the burning behaviour of this fuel package. Events 1 to 3 are typically found in the pyrolysis regime, with the process of flame spread up the backrest as a transition to the flaming regime. Similarly, the backrest collapse marks the transition to the smouldering regime with events 6 to 8 mainly occurring during this latter period. The following sections will present the results across all trials using the events and global regimes to characterize the burning behaviour.

4.2. Results Across All Trials

The combined mass loss rate (MLR) and heat release rate (HRR) result of each individual trial are presented in Fig. 5 as a median, interquartile range, and total range. Given the relationship between HRR and MLR, they exhibit similar trends in time. Of particular note from these plots is that the widest scatter is observed during the flaming regime (approximately 200 s to 600 s); this period is associated with the maximum of visually observed flaming, and the occurrence of the peak HRR. It is also notable that the interquartile range reduces during the smouldering regime.

Although presenting the data in this way can be useful for visualising the scatter, the presented median value for HRR obscures the transient influence of the key events. For example, when considering only the median in time, the rapid growth rate associated with the burn-through of the backrest is smeared across the 25 different trials. The median time series therefore gives a peak HRR of only 160 kW, compared to a mean peak of 215 kW across all trials. As such the med-

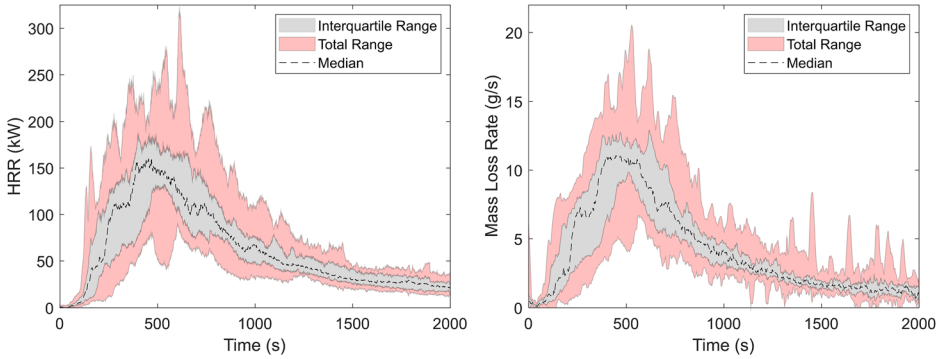

Figure 5. HRR and MLR data for each of the 25 trials conducted. Figures show the total ranges, interquartile ranges, and medians for each data set.

ian of the time series does not accurately portray key characteristics of any individual trial. The median of the time series data is not, therefore, a useful metric by which to represent the burning behaviour of the upholstered chair used in this study.

5. Analysis

The results from all 25 trials indicate that linking recorded data to key events is vital in characterizing the relevant physical drivers of the burning process. The following section will explore the results in more detail and present further analyses of both the events and recorded data.

5.1. Emission Yields and $\Delta H_{c,eff}$

As described previously, the yield for any given species can be calculated taking the mass generation of that species, $\dot{m}_i$ divided by the time resolved MLR. Figure 6 presents the CO_2 and CO yield, for each trial. The effective heat of combustion ($\Delta H_{c,eff}$) is also determined using the MLR time series — in this case, the numerator being the HRR.

Data for the CO_2 yield and $\Delta H_{c,eff}$ show growth in the early phase of each trial and a transition to relatively steady behaviour throughout most of the remaining duration. The transition to a steady CO_2 yield and $\Delta H_{c,eff}$ is due to the similar trends in the HRR, MLR, and CO_2 data. During the period of steady flaming (i.e., approximately 350 s to 1500 s) the CO_2 yield and $\Delta H_{c,eff}$ was approximately 1.52 g/g $\pm$ 0.50 g/g and 14.20 kJ/g $\pm$ 4.55 kJ/g where the $\pm$ range is determined from the interquartile range. These values are comparable to those found in literature for PU foam and wood [33].

The CO yield, however, follows a characteristically different behaviour. The observed transience can be directly linked to the three burning regimes identified in Sect. 4.1. The initial increase in CO yield is associated with the initial period of

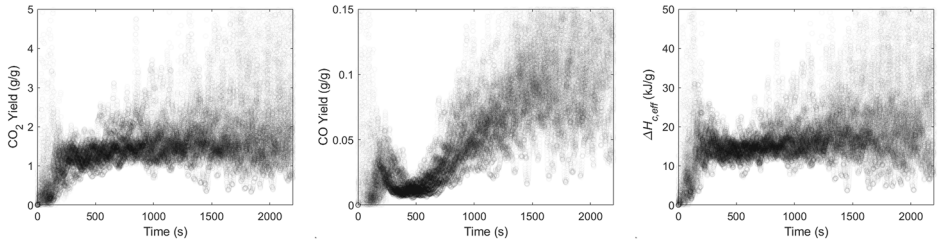

Figure 6. Time resolved CO_2 yield, CO yield, and $\Delta H_{c,eff}$ presented both as individual time series.

high rates of pyrolysis without significant flaming. This period is followed by a decline in CO yield as more of the gaseous species are oxidized in the flame (i.e. the flaming regime). The CO yield then increases as the remaining debris smoulders. The anticipated CO yield of PU foams based on standardized test methods range from 0.01 g/g to 0.05 g/g (depending on the composition of the foam) [33]; the results from the upholstered chairs in this study, however, highlight the transience in CO yield over the duration of the experiment. The use of the CO yields presented in literature (e.g., 0.01 g/g to 0.05 g/g) would result in a significant under-prediction in the CO generation of these experiments. Therefore, a constant CO yield value cannot accurately characterize the CO generation observed in these experiments.

Figure 7 shows the yields for methane (CH_4) and the nitrogen containing species likely to be present in the generated emissions; nitrogen monoxide, nitrogen dioxide and hydrogen cyanide (NO, NO_2 and HCN). No single specie presented in Fig. 7 displays a steady yield. Each yield was found to be transient and the trends shown by the yields reported in Fig. 7 largely mirror the transition between global burning regimes as discussed in Sect. 4.1.

Each of the four species presented Fig. 7 show an initial peak during the pyrolysis stage, followed by a decline during flaming, mirroring the trends previously seen for CO. In the case of NO_2, CH_4, and HCN, the yields approach zero during flaming. The decrease of each yield during flaming is driven by the oxidisation of each species by the flame (as discussed previously with CO). The NO yields consistently displays a non-zero value in the yield data during the flaming regime. This is due to the high temperatures required to further oxidize NO [39, 40], resulting in large quantities of NO escaping the flame sheet.

HCN is a commonly tracked species due to the hazard it poses to building occupants [41, 42]. Some individual trials displayed instantaneous HCN yields as high as 0.02 g/g during the pyrolysis regime. However on average, the initial HCN yield obtained during the pyrolysis presented align with the HCN yields obtained from small scale studies on the combustion of foams ($\sim$0.006 g/g to 0.007 g/g) [43]. HCN was detected during the pyrolysis stage of the experiments and again, to a lesser degree, during the smouldering regime; HCN was not seen in large quantities during flaming.

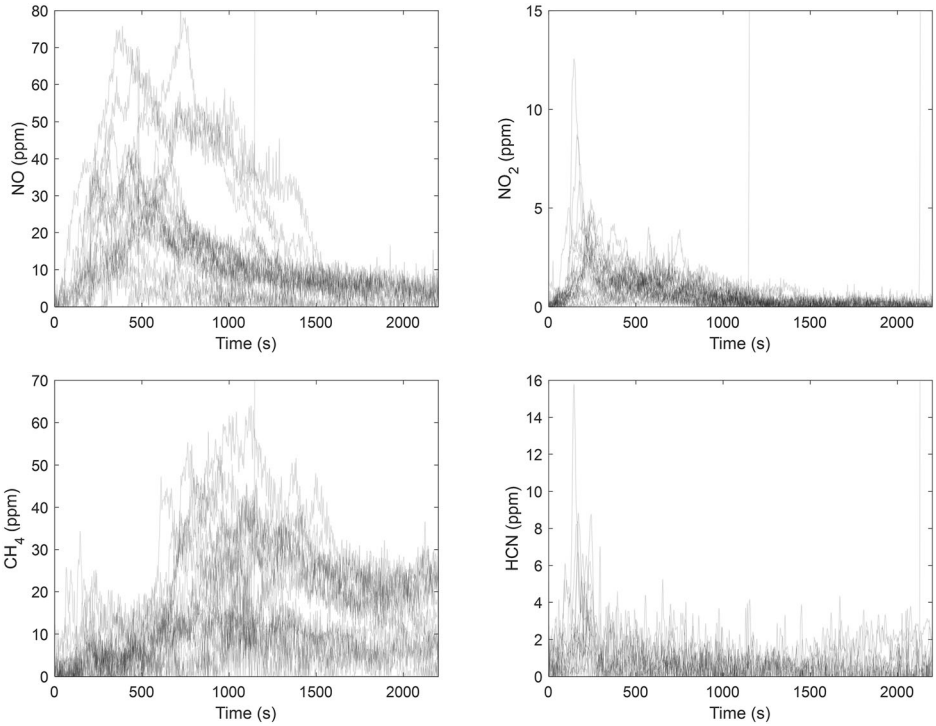

Figure 7. Time resolved yields for NO, NO_2, CH_4, and HCN for each trial.

As the experiments transition from flaming to smouldering, both the NO and CH_4 yields were found to increase. CH_4 has been used in previous studies as a surrogate for inefficient pyrolysis or the presence of smouldering in biomass [44, 45]; as such the increase in CH_4 yield is expected both in the pyrolysis regime and as the experiments transition to the smouldering regime.

5.2. Key Events

As previously described, key events throughout the each trial were found to drive trends in the recorded data. The time of these events was recorded for each trial (Fig. 8). These results show that, as the fire progresses, the time history of the burning behaviour is increasingly influenced by past events. On average, the range of observed times increases with each subsequent event (i.e. a delay to the back-rest burn-through, will also delay the collapse of the base). Figure 8 also illustrates the distribution of the HRR at the moment of each event. This allows the median HRR at each event to be identified.

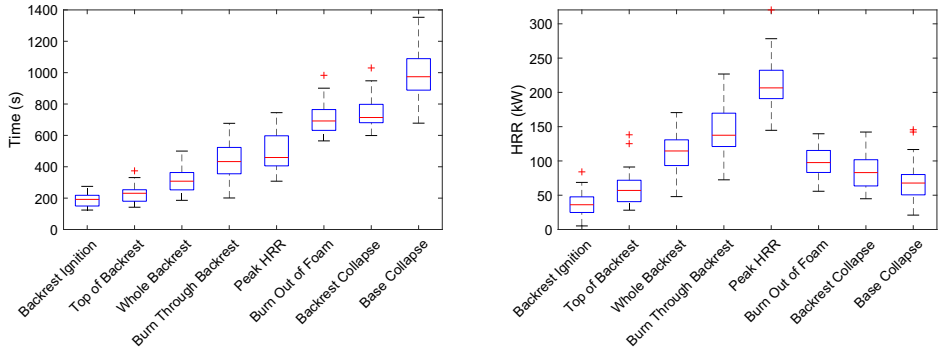

Figure 8. Time of each event, and corresponding HRR at each event.

5.3. Normalized Heat Release Rate

Analysis of the HRR data showed that the median value in time obscured changes associated with stochastic events (see Fig. 5). No single trial is expected to burn in a manner reflected by the median in time. The median presented in this way, therefore, becomes meaningless in describing the transient behaviours that occur during the burning of a complex fuel package.

To generate a more physically relevant understanding of the burning behaviour, the idea of "normalizing" the heat release rate is introduced. The normalization process used here incorporates the time at which specific events occur, thereby aligning each dataset to align with key events instead of time. This process generates a "fictional" data series that is useful in identifying the causal relationship between key events and fire behaviour.

To create these "event resolved HRR curves", the time of each event is used to separate each dataset into sections. These separated curves were then normalised with respect to the time elapsed between each event. This produces a set of HRR curves where the events occur in synchrony along the x-axis (Fig. 9). In this plot, the median curve is much more representative of each individual HRR curve observed in this study than the time resolved median (as seen in Fig. 5). The interquartile range is also significantly reduced compared to the data presented in Fig. 5. Within the interval between removal of the burner and backrest collapse, the interquartile range reduced from an average of 66 kW (Fig. 5) to approximately 34 kW (Fig. 9)—a reduction of nearly 50%. While presenting the data in this way significantly reduces the variability in the HRR data, the data is no longer presented as a time series and therefore loses direct applicability in many fire engineering analyses. A user could, however, use the time distributions of each key event to probabilistically determine HRR curves to be used in analysis (notwithstanding potential issues with conservation of mass and energy). It should be noted that only a select number of events from Table 2 are used in Fig. 9; this was done to highlight some of the key mechanisms controlling the fire behaviour, however this process could be done with more or less key events so long as the relevant physical drivers are identified.

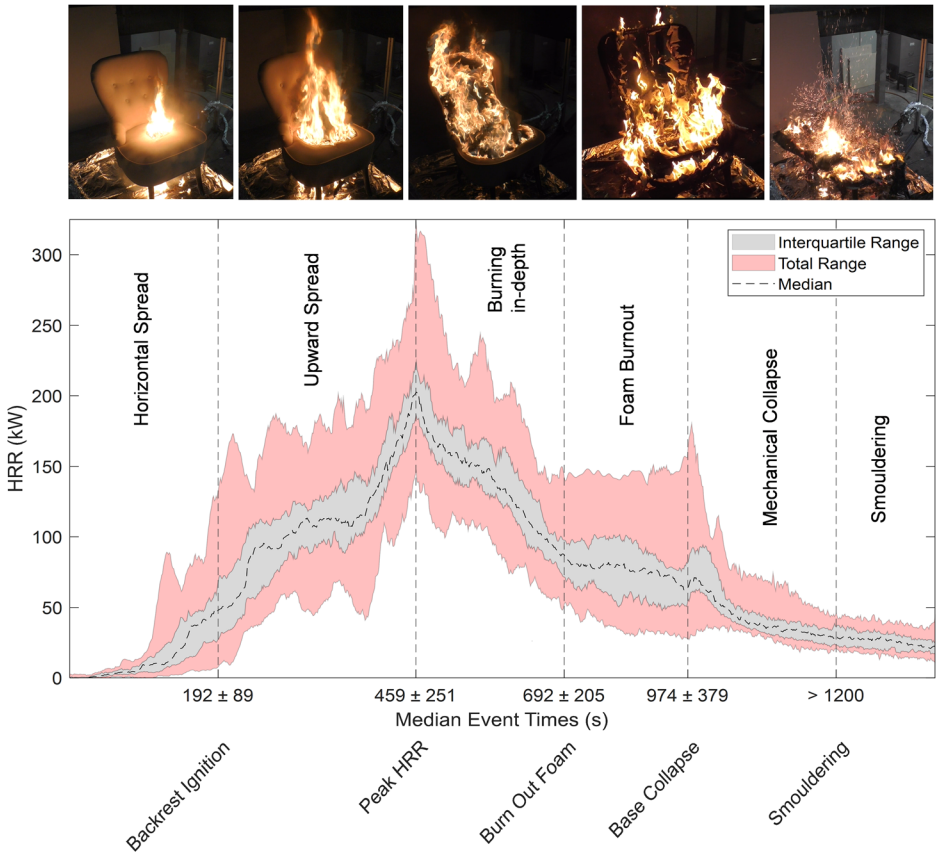

Figure 9. Normalized heat release rate based on key events. Each period of time between key events is dictated by different physical phenomena. Median times for each event are also presented with ± values approximate the range in event time seen previously in Fig. 8. It should be noted that each distribution of times is non-uniform (i.e., non-Gaussian); the use of a uniform range is an approximation for visualization purposes.

The core value of this normalization exercise lies in the ability to collapse data based on physical events; behaviour that would otherwise be seen as random variation can be attributed explicitly to key physical processes. Presented as a normalized curve, the periods of HRR between key events can be linked to the phenomena driving the burning rate. Between the start of the experiment and the ignition of the backrest, the growth in HRR is controlled by the process of horizontal flame spread along the seat cushion. After the backrest ignited, fire growth is then controlled primarily by upward flame spread along the backrest. Beyond the peak HRR, the burning rate is controlled by the rate of burning into the depth of the chair assembly instead of flame spread. Eventually the foam then

begins to burn out and the remaining HRR behaviour is dictated by the mechanical collapse (resulting in a local maximum in HRR) and smouldering of the OSB frame. The exact onset of smouldering can prove difficult to define on this scale, therefore the transition of > 1200 s indicated in Fig. 9 represents an approximate transition to primarily smouldering observed across all trials.

Characterizing the HRR using the key mechanism of growth/decay (e.g., horizontal spread, upward spread) provides context to generalizing the HRR results of any fire test. For the results seen in Fig. 9, the growth from the start of the experiment to the peak HRR is dictated by two distinct regimes of flame spread. These two forms of flame spread display characteristically different rates of spread [46, 47], and therefore two characteristically different effects on the HRR growth. To describe these two stages using the same mathematical model would ignore the transition between the two processes; the HRR would be more accurately described by separating these distinct regimes. Identifying these mechanisms of growth (e.g., horizontal vs upward spread) is critical in meaningfully generalizing the HRR of any complex fuel package such as vehicle fires or compartment fires (e.g., [48]).

6. Discussion

These results highlight the range of variability in time resolved data even under a well-constrained fire testing scenario. The normalized burning rate data presented in Fig. 9 shows that insight can be gained by identifying key events and physical process that dictate the time resolved burning rate. While this normalized curve presents an interesting theoretical discussion (i.e., illustrates the cause and effect of physical occurrences), the reality is that data must often be practically applied as a time series.

Therefore if an engineer wishes to use experimentally determined HRR data as an input to further analysis (e.g., CFD modelling), then a decision must be made regarding the best way to characterize the observed variation. The use of a mean or median value across multiple trials in time has been shown to create an unrealistic picture of the transient burning rate — and under-predict the peak behaviour and growth rates (Fig. 5). A user could alternatively envelope the entire curve with the maximum time between each event; this would likely be conservative (i.e., more energy would be released), but would result in an approximation which also no longer resembled the reality of the item burned. Alternatively, one could use time and HRR data seen in Fig. 8 input distributions for probabilistic analysis or as bounds for structural design optimization (e.g., [49–51]). The development of large data sets for other fire safety experiments (e.g., compartment fires, ceiling jets, heat fluxes from fires) would therefore better capture the relevant bounds of certainty for such optimization techniques.

Species emissions and yields are often presented in experimental studies and used in engineering applications (e.g., CO yields, soot yields). As mentioned previously, yields for a variety of species are often presented as a constant (e.g., a CO yield of 0.024 g/g for PMMA [33]). While yield results for CO_2 and $\Delta H_{c,eff}$ in this

study display a relatively constant behaviour over much of the experiment, each showed a transient behaviour early on in the experiment during the pyrolysis phase. Even when considering the periods over which these yields show a constant behaviour, there remains a large degree of scatter around the mean. Neither the early transience nor large degree of scatter are captured by the use of an average, constant yield.

Other species yields (CO, NO, NO_2, CH_4, and HCN) exhibited more variable behaviour. The CO yield displayed a highly transient behaviour with a high yield during pyrolysis and smouldering and a decrease in yield during flaming. The CO yield began to rise even while flaming was still occurring over large areas of the chair (i.e., while the HRR remained relatively high); this indicates that the transition between the flaming and smouldering regime is gradual and cannot be defined by a single instant in time. To use a constant CO yield within a model would not reflect the behaviour observed in these experiments. It is therefore suggested that when applying yields in practical scenarios the use consider the different regimes that may occur in the scenario being simulated (i.e., pyrolysis, flaming, smouldering) to avoid an underestimation of species such as CO.

7. Conclusions

A total of 25 repeat trials were conducted using a commercially available upholstered chair to compare the variation in burning rate and gaseous emissions. Data presented as a time series across the 25 trials illustrated a substantial degree of scatter. Nevertheless, there was a high degree of commonality between the trials in terms of the key physical events and the regimes of burning. In summary, it was found that:

1. Conventional averaging (i.e., median in time) techniques masked the commonality between the trials. Close examination revealed notable similarity in terms of the progression of each fire, but this insight is lost if relying only on a median value in time. Careful consideration is required when characterizing average behaviour for complex fuel packages.
2. The time resolved burning behaviour of upholstered furniture is tied to physical drivers and that these events were common to all the experiments.
3. Three regimes of burning were observed—pyrolysis, flaming, and smouldering. Emissions data can be used to characterize these regimes.
4. The generation of gaseous species is often modelled using a constant yield; species yields are not constant over the duration of each trial and are strongly linked to the identified burning regimes.

Findings from this work are inherently limited to both the upholstered chair and the ignition method used. Changes in the experimental procedure will result in different burning behaviour; the influence of such changes on the fuel package studied here will be the subject of future publications. However, the general observations regarding the observed burning regimes and the process of linking physi-

cal events to burning behaviour are applicable beyond the conditions studied here. The burning of complex fuel systems such as upholstered furniture will inevitably display stochastic variation as complexity and scale increases. When studying such systems, it is useful to consider key physical events and the influence of these events on the burning behaviour. The number of trials performed in this study has allowed this link to be made and analysed. It is recommended that those who may apply such data as an input to engineering applications also consider the intrinsic variability in such data to fully understand the range of possible error in subsequent analysis. The results presented in this work can be used to provide context to the range of variation possible for researchers developing experimental programs or practitioners using such data in engineering applications.

Acknowledgements

The authors would like to thank the SFPE Foundation for their financial support in providing David Morrisset an SFPE Student Research Grant. Additionally, the authors would like to acknowledge the technical and financial support of the Edinburgh Fire Research Centre. We would also like to thank Prof. Jose Torero for his discussion of the experimental procedure and analysis in this study, and both Prof. Richard Emberley and Prof. Glen Thorncroft for their discussion on statistical variation.

Declarations

Competing Interests No potential competing interest was reported by the authors.

Open Access

Appendix: Selection of MLR Smoothing Filters

Previous studies have shown that the method used to process MLR data, namely the smoothing technique used, can significantly skew the smoothed MLR data. High degrees of smoothing have been shown to result in significant reductions in localized peak values and can result in temporal shifts [29, 38]. In order to mitigate these effects in this study, the following analysis was conducted in the selection of a smoothing filter. Further information of the filters used in this section can be found elsewhere [29, 38, 52–54].

Morrisset et al. present a method based on the conservation of mass to determine the most appropriate representation of the MLR based on the recorded mass time history [29]. The approach is described in Eq. 1 and Fig. 10. The principle of this method being based comparing the difference in recorded mass between t_o and t_n, $\Delta m = m_o - m_n$, to the integrated MLR over the same time interval, $\int_{t_o}^{t_n} \dot{m} dt$. A smoothing filter can then be chosen by comparing Δm to $\int_{t_o}^{t_n} \dot{m} dt$ over the duration of the experiment (i.e., finding a filter with minimal variation from the actual observed mass loss).

$$m_o - m_n = \Delta m \approx \lim_{\Delta t \to 0} \sum_{i=1}^{n} \dot{m} \Delta t = \int_{t_o}^{t_n} \dot{m} dt \tag{1}$$

$$\Gamma = \frac{\Delta m - \int_{t_o}^{t_n} \dot{m} dt}{\Delta m} \tag{2}$$

All raw MLR data in this study was differentiated using a forward difference then smoothed with a filter. As seen in previous studies, high smoothing windows result in the truncation of localized peaks in the MLR data. While low filter windows, display noise on the scale of the raw MLR data and therefore does not provide a

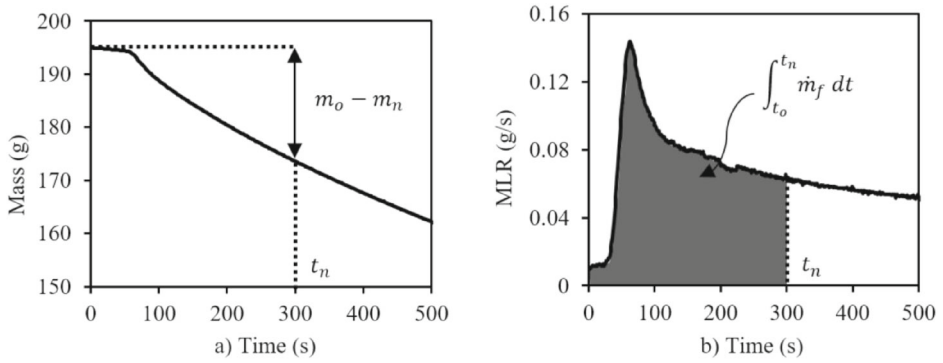

Figure 10. A graphical representation of the integral goodness-of-fit method, where the integrated MLR data between t_o and t_n should be approximately equal to $m_o - m_n$.

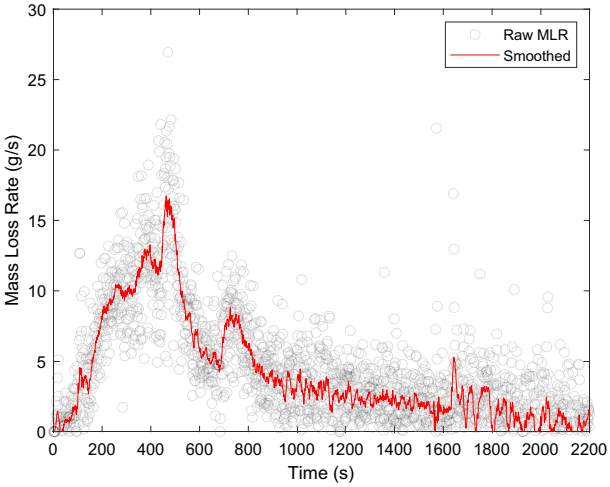

Figure 11. The chosen smoothing filter used in this study for MLR data (a Saviztky-Golay filter with a frame width of 25 and a 3rd order polynomial) presented alongside the raw MLR data taken from the time derivative of the recorded mass.

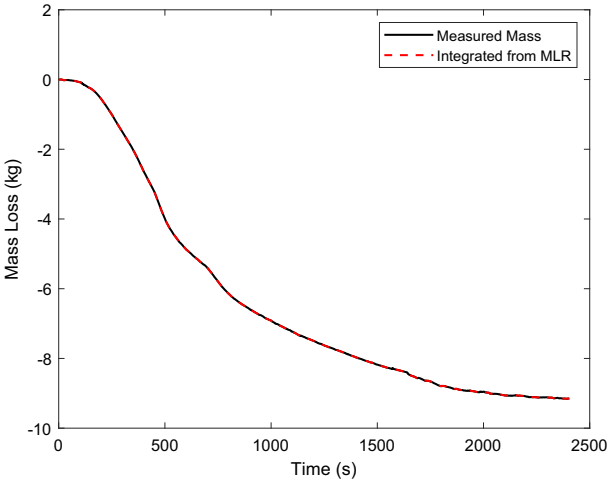

Figure 12. Both the experimentally measured mass loss curve from the experiment and the reconstructed mass loss from the integration of the MLR as seen in Eq. 1 and Fig. 10.

continuous representation of the MLR. The filter can be selected based on the integration technique seen in Fig. 10.

The selected filter for this study (Savitzky–Golay with a frame width of 25 and a third order polynomial) can be seen along with the raw MLR data in Fig. 11. This smoothing filter to optomize maintiang a $\Gamma < 1\%$ while providing enough smoothing to produce species yields that displayed meaningful trends without further smoothing. The degree to which the smoothed curve represents the true mass loss behaviour is further captured in Fig. 12 which compares the experimentally measured mass loss and a reconstructed mass loss from the integrated smoothed MLR.

References

1. Ohlemiller TJ, Villa KM (1990) Furniture flammability: an investigation of the California Bulletin 133 Test. Part II: characterization of the ignition source and a comparable gas burner (NISTIR 4348). National Institute of Standards and Technology
2. California Technical Bulletin TB133. Flammability test procedure for seating furniture for use in public occupancies
3. Babrauskas V (1979) Full-scale burning behavior of upholstered chairs, vol 1103. Department of Commerce, National Bureau of Standards
4. Babrauskas V, Lawson JR, Walton WD, Twilley WH et al (1982) Upholstered furniture heat release rates measured with a furniture calorimeter
5. Enright T (1999) Heat release and the combustion behaviour of upholstered furniture
6. Babrauskas V (2016) The cone calorimeter. In: SFPE handbook of fire protection engineering. Springer, pp 952–980
7. Morrisset D, Thorncroft G, Hadden R, Law A, Emberley R (2021) Statistical uncertainty in bench-scale flammability tests. Fire Saf J 122:103335
8. Morrisset D, Thorncroft G, Hadden R, Law A, Emberley R (2021) Sequential analysis for quantifying statistical uncertainty in fire testing. In: 12th Asia-Oceania symposium on fire science and technology
9. Babrauskas V (2016) Heat release rates. In: SFPE handbook of fire protection engineering. Springer, pp 799–904
10. Thompson AL, Kim I, Hamins A, Bundy M, Zammarano M (2022) Performance and failure mechanism of fire barriers in full-scale chair mock-ups. Fire Mater 46(1):329–346
11. Babrauskas V, Krasny JF (1985) Fire behavior of upholstered furniture. Final Rep. Natl. Bur. Stand.
12. Babrauskas V (1983) Upholstered furniture heat release rates: measurements and estimation. J Fire Sci 1(1):9–32
13. Bwalya A, Gibbs E, Lougheed G, Kashef A (2015) Heat release rates of modern residential furnishings during combustion in a room calorimeter. Fire Mater 39(8):685–716
14. Hofmann A, Klippel A, Gnutzmann T, Kaudelka S, Rabe F (2021) Influence of modern plastic furniture on the fire development in fires in homes: large-scale fire tests in living rooms. Fire Mater 45(1):155–166
15. Kerber S (2012) Analysis of changing residential fire dynamics and its implications on firefighter operational timeframes. Fire Technol 48(4):865–891
16. Pau DSW, Fleischmann CM, Delichatsios MA (2020) Thermal decomposition of flexible polyurethane foams in air. Fire Saf J 111:102925

17. Liu C, Zong R, Chen H, Wang J, Wu C (2019) Comparative study of toxicity for thermoplastic polyurethane and its flame-retardant composites. J Thermoplast Compos Mater 32(10):1393–1407
18. Morgan AB (2021) Revisiting flexible polyurethane foam flammability in furniture and bedding in the United States. Fire Mater 45(1):68–80
19. Zammarano M et al (2020) Reduced-scale test to assess the effect of fire barriers on the flaming combustion of cored composites: an upholstery-material case study. Fire Mater 45(1):114–126
20. Zammarano M et al (2020) Full-scale experiments to demonstrate flammability risk of residential upholstered furniture and mitigation using barrier fabric
21. Pitts WM et al (2021) Effects of upholstery materials on the burning behavior of real-scale residential upholstered furniture mock-ups. Fire Mater 45(1):127–154
22. Zammarano M (2021) Fire performance of upholstery materials: correlation between cube test and full-scale chair mock-ups. Technical Note (NIST TN), National Institute of Standards and Technology
23. Kim I et al (2022) Demonstration of an all-in-one solution for fire safe upholstery furniture: a benign backcoating for smoldering and flame-resistant cover fabrics. Fire Mater 46(4):677–693
24. NIST Fire Calorimetry Database (FCD)
25. Zulmajdi IU, Tohir MZM, Yaw TCS, Harun MY, Said MSM (2023) Distribution of probabilistic design fires for single residential items. Fire Saf J 140:103908
26. Melcher T, Zinke R, Trott M, Krause U (2016) Experimental investigations on the repeatability of real scale fire tests. Fire Saf J 82:101–114
27. Janssens ML (1991) Measuring rate of heat release by oxygen consumption. Fire Technol 27(3):234–249
28. Quintiere J (2006) Fundamentals of fire phenomena. Wiley, Chichester
29. D. Morrisset, S. Santamaria, R. M. Hadden, and R. Emberley, "Implications of Data Smoothing on Experimental Mass Loss Rates," *Fire Saf. J.*, no. 103611, 2022.
30. Morrisset D, Schmidt L, Law A, Hadden RM (2023) Carbon monoxide and carbon dioxide generation of timber during pyrolysis, flaming, and char oxidation. In: 11th European combustion meeting
31. Boonmee N, Quintiere JG (2005) Glowing ignition of wood: the onset of surface combustion. Proc Combust Inst 30(2):2303–2310
32. Morrisset D, Hadden RM, Bartlett AI, Law A, Emberley R (2021) Time dependent contribution of char oxidation and flame heat feedback on the mass loss rate of timber. Fire Saf J 120:103058
33. Hurley MJ et al (2015) Appendix 3: Fuel properties and combustion data. In: SFPE handbook of fire protection engineering, pp 3437–3475
34. Wekegrzyński W, Vigne G (2017) Experimental and numerical evaluation of the influence of the soot yield on the visibility in smoke in CFD analysis. Fire Saf J 91:389–398
35. Bryant RA, Mulholland GW (2008) A guide to characterizing heat release rate measurement uncertainty for full-scale fire tests. Fire Mater An Int J 32(3):121–139
36. Janssens ML et al (2012) Reducing uncertainty of quantifying the burning rate of upholstered furniture. Final Rep. Award, no. 2010-DN
37. Guillaume E, de Feijter R, van Gelderen L (2020) An overview and experimental analysis of furniture fire safety regulations in Europe. Fire Mater 44(5):624–639
38. Morrisset D, Santamaria S, Law A, Hadden RM (2022) Towards an improved processing methodology for mass loss rate data in fire testing procedures. In: Symposium on obtaining data for fire growth models—STP1642

39. Wünning JA, Wünning JG (1997) Flameless oxidation to reduce thermal no-formation. Prog Energy Combust Sci 23(1):81–94
40. Hayhurst AN, Vince IM (1980) Nitric oxide formation from N2 in flames: the importance of 'prompt' NO. Prog Energy Combust Sci 6(1):35–51
41. Tabian D et al (2021) Toxic blood hydrogen cyanide concentration as a vital sign of a deceased room fire victim—case report. Toxics 9(2):36
42. Higgins EA, Fiorca V, Thomas AA, Davis HV (1972) Acute toxicity of brief exposures to HF, HCl, NO_2 and HCN with and without CO. Fire Technol 8:120–130
43. Stec AA, Hull TR (2011) Assessment of the fire toxicity of building insulation materials. Energy Build 43(2):498–506
44. Olsson M, Ramnäs O, Petersson G (2004) Specific volatile hydrocarbons in smoke from oxidative pyrolysis of softwood pellets. J Anal Appl Pyrolysis 71(2):847–854
45. Jayakumar A et al (2023) Systematic evaluation of pyrolysis processes and biochar quality in the operation of low-cost flame curtain pyrolysis kiln for sustainable biochar production. Curr Res Environ Sustain 5:100213
46. Ito A, Kashiwagi T (1988) Characterization of flame spread over PMMA using holographic interferometry sample orientation effects. Combust Flame 71(2):189–204
47. Fernandez-Pello AC, Hirano T (1983) Controlling mechanisms of flame spread. Combust Sci Technol 32(1–4):1–31
48. Brzezinska D, Ollesz R, Bryant P (2020) Design car fire size based on fire statistics and experimental data. Fire Mater 44(8):1099–1107
49. Franchini A, Galasso C, Torero JL (2023) Optimising the inherent fire capacity of structures. Fire Saf J 141:103883
50. Cadena JE, Osorio AF, Torero JL, Reniers G, Lange D (2020) Uncertainty-based decision-making in fire safety: analyzing the alternatives. J Loss Prev Process Ind 68:104288
51. Magnusson SE (1997) Risk assessment. In: Fire safety science—proceedings of the fifth international symposium, pp 41–58
52. Savitzky A, Golay MJE (1964) Smoothing and differentiation of data by simplified least squares procedures. Anal Chem 36(8):1627–1639
53. Bromba MUA, Ziegler H (1981) Application hints for Savitzky-Golay digital smoothing filters. Anal Chem 53(11):1583–1586
54. Staggs JEJ (2005) Savitzky-Golay smoothing and numerical differentiation of cone calorimeter mass data. Fire Saf J 40(6):493–505